

Endogenous miR-21 and TIMP-1 Regulate Hepatic Injury and Fibrosis by Bile Duct Ligation in Vivo

Chung-Hsin Lee

TVGH: Taichung Veterans General Hospital

Yi-Chin Yang

Taichung Veterans General Hospital Puli Branch

Yi-Wen Hung

Central Taiwan University of Sciences and Technology

Ching-Chang Cheng

China Medical University

Yen-Chung Peng (✉ pychunppp@gmail.com)

Taichung Veterans General Hospital Chiayi Branch <https://orcid.org/0000-0002-8993-3039>

Research Article

Keywords: Bile duct degeneration, Common Bile Duct Ligation, Liver fibrosis, TIMP metallopeptidase inhibitor 1

Posted Date: March 30th, 2021

DOI: <https://doi.org/10.21203/rs.3.rs-338885/v1>

License:   This work is licensed under a Creative Commons Attribution 4.0 International License.

[Read Full License](#)

Abstract

TIMP metalloproteinase inhibitor 1 (TIMP-1) has been identified as a multifunctional molecule with divergent functions. It participates in wound healing and regeneration, cell morphology and survival, tumor metastasis, angiogenesis, and inflammatory responses. An imbalance of Matrix Metalloproteinase/TIMP regulation has been implicated in several inflammatory diseases. TIMP-1 could be considered an important regulator in the process of liver fibrosis and bile duct degeneration. Thus, we aimed to determine the role of TIMP-1 in a rat model of Common Bile Duct Ligation (CBDL). Male Sprague-Dawley rats were divided into several groups, including those with/ without CBDL surgery and those with/without amiodarone or simvastatin administration. Amiodarone/simvastatin treatment was given at a daily dose of 15 mg/kg and 18 mg/kg by means of intergalactic gavage, which began 7 days prior to CBDL induction. Two weeks after surgery, the animals in each group were sacrificed and hepatocyte degeneration severity was examined using histological morphologies. Large-scale array for secretory factors is intended for the purpose of finding key functional protein after CBDL. The hepatic level of miR-21 was determined through Taqman miRNA analysis. Furthermore, the TIMP-1 level in liver tissue was also visualized by histological stain. Liver injury and fibrosis were founded in CBDL rats based upon histopathological examination and serum biochemical analysis. Hepatic miR-21 and TIMP-1 were significantly up-regulated in CBDL rats, while being slightly rescued in response to amiodarone or simvastatin treatment. Up-regulation of miR-21 and TIMP-1 may result in the progression of hepatic cirrhosis after bile duct obstruction. Drug intervention for cirrhosis, like the use of statin, may function via similar mechanisms.

Introduction

During the process of chronic liver disease, fibrosis results from the accumulation of extracellular matrix proteins, which may contribute to severe sequels such as liver failure, and portal hypertension. [1] Being a serious issue, liver fibrosis is also associated with an increased risk of cirrhosis and liver cancer. Therefore, determining the putative factors which may apply as a prevention strategy for liver fibrosis and any associated clinical events is important. Liver fibrosis is a complicated and multi-factorial related process. Several types of cells, cytokines and miRNAs have been reported to be involved in the initiation and progression of liver fibrosis and carcinogenesis.[2-4] Surgical ligation of the Common Bile Duct (CBDL) has become the most commonly used animal model to induce obstructive cholesteric injury. Through this type of study, the molecular and cellular events underlie these pathophysiological mechanisms induced by inappropriate bile flow.[5-7] In the present study, we aim to identify the functional secretory proteins or miRNAs which are involved in the progression of hepatic fibrosis or carcinogenesis in a rat model of CBDL.

The family of Tissue Inhibitor of Matrix Metalloproteinase (TIMPs) (1-4) plays a central regulatory role as inhibitors of Matrix Metalloproteinase (MMPs), which are enzymes involved in extracellular matrix maintenance and remodeling. Recently, TIMP-1, which is the inducible form of TIMPs, has been identified as a multifunctional molecule with divergent functions, including tissue repair and tissue remodeling. It

participates in wound healing and regeneration, cell morphology and survival, tumor metastasis, angiogenesis, and inflammatory responses.[6] An imbalance of MMP/TIMP regulation has been implicated in several inflammatory diseases. In the process of liver fibrosis and bile duct regeneration, as a result of recurrent healing and regeneration, TIMP-1 could thus be considered as providing an important role. Additionally, there are several cytokines or signaling pathways which could regulate the pathogenesis of hepatic fibrosis by inducing TIMP-1 expression.[8-10]

It is known that microRNAs (miRNA) are also involved in this process of liver fibrosis and hepatocarcinogenesis.[11-13] In a tissue study for liver tumor, miR-21, miR-31, miR-122, miR-221, miR-222 were significantly up-regulated in HCC tissues, while miR-122, miR-145, miR-200c, miR-221, and miR-222 were all down-regulated.[14] Additionally, expression of miR-21, miR-31, miR-122, and miR-221 in HCC correlated with cirrhosis, while miR-21 and miR-221 were associated with tumor stage and poor prognosis. Also, miR-21 plays an important role in inflammation, as well as the process of liver inflammation and carcinogenesis.[15]

There have been reports that miRNA attends the process of liver fibrosis, and could regulate TIMP-1 in hepatic or non-hepatic fibrosis, as well as in carcinogenesis.[16-20] Circulating miR-21 is known to be aberrantly expressed in HCC, which implies that miR-21 is a promising and novel indicator of HCC. Therefore, miR-21 may serve as a potential co-biomarker for early-stage HCC diagnosis.[21] However, data regarding the functions of miR-21 and its correlation to TIMP-1 in liver fibrosis are limited.[22, 23]

To investigate the role of miR-21 and TIMP-1 in liver inflammation, we performed liver injury using a CBDL model in rats, and evaluated the role of these molecules in the process of CBDL.

Materials And Methods

Bile duct ligated rats

Animal study was performed under the approval of the Institutional Animal Care and Use Committee (IACUC) of our institution (Approval No. La-1071565). Thirty-six male Sprague-Dawley (SD) rats were purchased from BioLASCO Taiwan Co., Ltd.

Initially, these rats were housed 3 per cage, allowed free access to water and food, while being maintained under both a constant temperature (23 ± 1 °C) and humidity level ($60 \pm 10\%$), during a 12-h light/dark cycle. For bile duct ligation, a double ligation of the bile duct (proximal and distal sites) was performed under the inhalation of 2.0-3.0% isoflurane. For comparison, in sham-operated rats the bile duct mobilized but not ligated. Vitamin K (50 mcg SC) was administered subcutaneously each week. After bile duct ligation or sham operation, the rats were randomly divided into 6 groups (n=6): Sham, Sham + simvastatin, Sham + amiodarone, CBDL, CBDL + simvastatin, and BDL + amiodarone. Drugs were grinded and suspended using 0.5% Carboxymethyl Cellulose (CMC) solution prior to gavage (atorvastatin 1.5 mg/ml, amiodarone 1.8 mg/ml). The rats were pretreated with atorvastatin (15 mg/kg body weight per day) and amiodarone (18 mg/kg/day) 1 week prior to their BDL operation, and

continuing until 3 weeks post-operation. The sham and CBDL groups were administered a 0.5% CMC solution as a vehicle. Blood samples were collected once per week post-operation until the end point. After CO₂ euthanasia, the main organs were removed for examination and analysis.

Serum Biochemical function tests

Blood samples for biochemical analysis were collected from the tail veins under 1.5-2.0% isoflurane anesthesia at the 1st, 2nd and 3rd weeks post-operation. Blood samples were kept at room temperature for 1 hour and centrifuged at 3500 rpm for 20 minutes. The sera were then equally divided, with one stored at -70 °C and the other at 4 °C for the followed assays. The levels of serum Aspartate Aminotransferase (SGOT), Alanine Aminotransferase (SGPT), Alkaline Phosphatase (ALK-Pase), Total bilirubin (T-bilirubin), Creatinine and Blood Urea Nitrogen (BUN) were all analyzed for liver and renal function using an automated-analyzer (Hitachi, Model 736-60, Tokyo).[24]

Cytokine array

Cytokine array was examined in serum or tissue lysates samples according to the manufacturer's procedures taken from Rat Cytokine Array Panel A (R&D, USA & Canada). The nitrocellulose membrane, containing 29 different capture antibodies printed in duplicate, was blocked in Array Buffer 6 for one hour on a rocking platform shaker. While blocking, 1 mL of serum samples was added to 0.5 mL of Array Buffer 4 in separate tubes. That prepared sample then had 15 mL of reconstituted Detection Antibody Cocktail added to make a 100× dilution prior to being mixed well and incubated at room temperature for one hour. After replacing Array Buffer 6 with the sample/antibody mixtures, the NC membrane was incubated overnight at 2-8° C on a rocking platform shaker. After being washed twice with a wash buffer, the membrane was incubated with diluted Streptavidin-HRP for 30 minutes at room temperature. After washing out any excessive Streptavidin-HRP, the chemical reagent mix was carefully covered and the exposed membranes sent to X-ray film. After normalizing with negative control and reference spots, the density of expressed cytokines was compared between each group.

Histological assessment of hematoxylin-eosin staining

The main organs, fixed in 10% formalin, were processed through routine histology procedures, embedded in paraffin, and cut in 4 μm pieces. To determine the histopathological changes, the samples were stained with hematoxylin and eosin, which are used specifically for hepatocyte degeneration, bile duct proliferation and fibrosis. The tissues sections were then fixed in 4% paraformaldehyde for 24 hours and subsequently washed using Phosphate-buffered Saline (PBS). The next step was hydration, which was performed by soaking the samples sequentially in 100% and 95% ethanol solutions. The samples were soaked in each solution for 1 minute, before being washed under running water for 5 minutes. The excess water was removed from the samples, which were then immersed in a hematoxylin (Merck KGaA, Darmstadt, Germany) solution for 3 minutes to perform a nuclear staining. Following this, the samples were again washed under running water for 5 minutes and then immersed in an eosin (Sigma-Aldrich, Invitrogen, Carlsbad, CA, USA) solution for 1 minute to perform a nuclear staining. This was followed by

dehydration, during which the samples were soaked sequentially in 95%, and 100% alcohol solutions. The Hematoxylin-eosin (HE) stains were observed using an upright optical microscope (Nikon Eclipse E600 Nikon Corp., Tokyo, Japan), and their tissue morphology was photographed and recorded.[25] The criteria used for scoring hepatocyte degeneration severity were as follows: 0, normal; 1+, focal area; 2+, multifocal area; 3+, locally extensive area; and 4+, diffuse area.[26] The criteria used for scoring bile duct proliferation and fibrosis severity were as follows: 0, normal; 1+, bile duct proliferation and fibrosis present (extending from the portal triad region); 2+, mild proliferation and fibrosis (mild bile duct proliferation and collagen fiber present with extension, without compartment formation); 3+, moderate fibrosis (moderate proliferation and collagen fiber present, with some pseudo lobe formation); and 4+, severe fibrosis (severe proliferation and collagen fiber present, with thickening of the partial compartments, frequent pseudo lobe formation and bile duct proliferation).[27, 28] For the purpose of morphometric studies, liver fragments were taken from the left lobe of each rat. Fibrosis scores were given after the pathologist had thoroughly examined the three different areas in the tissue slides of each rat.

Immunohistochemical staining

The tissue slides were serially blocked with 0.3% H₂O₂/10% methanol in PBS for 10 min and 5% skim milk in PBS for 30 minutes. Subsequently, the tissue slides were incubated overnight at 4°C with mouse anti-TIMP-1 monoclonal antibodies (1:200, R&D Systems, Inc.). Therefore, a 3,3'-diaminobenzidine (DAB) brown color indicated TIMP-1. Subsequently, the sections were rinsed with PBS and incubated with a SuperPicture polymer detection kit (Invitrogen, Camarillo, CA, USA) for 10 minutes at room temperature, prior to being rinsed three times with PBS for 2 minutes. Finally, the sections were visualized by color development with a DAB enhancer (3, 3'-diaminobenzidine tetra hydrochloride, Fremont, CA, USA) and counterstained with hematoxylin. The immunostained sections were then examined using an optical microscope (Nikon Eclipse E600 Nikon Corp., Tokyo, Japan).

Small RNA extraction, reverse transcription, TaqMan™ real-time PCR

The isolation of small RNA was performed by PureLink™ miRNA Isolation Kit (Invitrogen, K157001). Briefly, 50 mg of liver tissue was homogenized by a tissue grinder and dissolved in TRIZOL reagent (Invitrogen, 15596018). After centrifuge at the maximal spin rate, the product was isolated through a two-step purification process, followed by incubation with different concentrations of ethanol. Finally, the small RNAs were further isolated according the manufacturer's instructions.

For the detection of mature miR-21 (Applied Biosystems, 00397), the small RNA mixture was reverse-transcribed using the TaqMan™ microRNA reverse transcription kit (Applied Biosystems, 4366596) in a reaction mixture containing a miRNA specific stem-loop reverse transcription primer. The quantification of mature miRNAs was performed using the TaqMan™ miRNA assay (Applied Biosystems, 4427975), which contained TaqMan™ probes in a universal PCR master mix without UNG (Applied Biosystems, 4440040). U6 small nuclear RNA (Applied Biosystems, 001973) was used as an internal control. The real-time PCR

reaction performed using TaqMan™ probes was conducted at 95° C for 10 minutes, and then 40 cycles at 95° C for 15 seconds and 60° C for 1 minute. The specificity of the reaction was verified through the melt curve analysis and the data was presented as $2^{-(\Delta\Delta Ct)}$.

Statistical analysis

The mean values and standard deviations relating to the measurement data for each group are presented. One-way Analysis of Variance (ANOVA) was used to determine if there were differences between the groups. The differences between the experimental and control groups were then analyzed using the independent samples t-test, with $P < 0.05$ indicating a statistically significant difference in the results.

Results

Biochemical tests of CBDL rats with or without drug treatment

Table 1 summarizes the results of the biochemical tests used in studying the rats. In comparison to the Sham group, CBDL induced common serum events of a liver biochemical test, such as SGOT (from 106.67 ± 13.20 to 347.17 ± 131.61 IU/L), SGPT (from 40.50 ± 4.76 to 92.17 ± 22.87 IU/L), ALK-Pase (from 274.17 ± 50.91 to 432.83 ± 106.59 IU/L) and bilirubin (from 0.01 ± 0.01 to 6.61 ± 3.42 mg/dL) at Week 1. These inductions seemed to be continued until 3 weeks after CBDL (**Figure 1**, $P < 0.05$). An anti-cirrhosis drug such as amiodarone could elevate SGOT, SGPT, and bilirubin one week after CBDL. However, a statin type drug like simvastatin did not induce these biochemical indicators. On the other hand, the serum creatinine levels, which may reflect renal functions, did not change due to CBDL or drug administration as well. These results indicate that liver functions reflected by biochemical analysis are impacted by CBDL, which is exerted even more through the use of amiodarone but not simvastatin.

Pathological results of CBDL animals

We further examined the severity of liver damage by visualizing hepatic tissue sections after performing standard Hematoxylin and Eosin stain (**Figure 2**). Fibrosis existed in CBDL-induced animals and showed a moderate to high degree of severity in the CBDL-only and CBDL + amiodarone groups (**Table 2**). However, the degree of fibrosis significantly decreased in the CBDL + simvastatin group in comparison with the CBDL only group ($p < 0.05$). In addition, mild necrosis and hepatocytic degeneration was found in CBDL-only rats but not CBDL + amiodarone rats. Thus, we concluded that CBDL exacerbates hepatic fibrosis, which can then be alleviated by simvastatin treatment in rat models.

Investigation of CBDL-associated cytokines

Next, we screened CBDL-associated cytokines using the antibody array approach in all serum samples. Four of 29 cytokines were selected as candidates. Amongst them, CINC-1, sICAM1 CD54, and TIMP-1 were up-regulated by CBDL; MIP-3 α was up-regulated by amiodarone alone; while CINC-1 and TIMP-1 were up-regulated by both CBDL and amiodarone treatments (**Figure 3**). Based upon both our results and

previous documentation, we have speculated that TIMP-1 may mediate the mechanism of fibrosis in a pathogenic liver found in CBDL animals.

TimP-1 expression in CBDL rats and the drug's effect

To investigate the role of TIMP-1 in CBDL animals, we attempted to verify the TIMP-1 expression by performing immunohistological stain. Our results show that TIMP-1 displayed a moderate expression level in a normal liver. After CBDL induction, its expression significantly increased in comparison to the non-CBDL group (**Figure 4**, $p < 0.05$). We showed that the TIMP-1 antibody offered only weak conjugation in liver tissue from SHAM group animals. However, its level in liver tissue was significantly enhanced in the CBDL group at the third week after bile duct ligation (DAB was brown). When the CBDL animals were fed with anti-fibrotic drugs for 2 weeks, the CBDL + AMI and CBDL + Statin groups effectively inhibited the level of TIMP-1, which was consistent with the SHAM + AMI and SHAM + Statin groups. After quantifying the staining diagram, it can be found that simvastatin did indeed offer more beneficial effects than amiodarone in regulating TIMP-1 expression in liver tissue after CBDL.

MiR-21 expression in CBDL rats and the drug's effect

Figure 5 shows that CBDL significantly induced the expression of miR-21 ($p < 0.05$). However, this induction could be suppressed by amiodarone and simvastatin. Simvastatin seemed to have stronger effects than amiodarone in inhibiting miR-21. Therefore, we deduced that miR-21 may participate in the pathogenic mechanisms of CBDL.

Discussion

Our results demonstrate that CBDL could induce a liver biochemical test, particularly GPT, GOT, Bilirubin and ALK-p. Additionally, the pathological results show that CBDL could induce biliary degeneration, liver necrosis and fibrosis as well. This may imply that there are possible risks of hepatic cell proliferation and tumorigenesis resulting from CBDL. Our results from histology and cytokine array indicate that TIMP-1 may be a crucial factor for CBDL-induced liver fibrosis. In addition, miR-21 was up-regulated by CBDL at the same time. Drug interventions, such as amiodarone and simvastatin which were used in this study, showed suppressive effects on CBDL-induced TIMP-1 and miR-21 expression respectively. However, we did not observe similar results when analyzing serum samples. This may be due to the multi-organ damage which occurred resulting from CBDL and certain drugs; and particularly that TIMP-1 was also resourced from multiple tissues.

Collectively, based upon our data, we have demonstrated that miR-21 and TIMP-1 may result in the progression of hepatic cirrhosis after bile duct obstruction. Use of drug intervention for cirrhosis such as statin, may function via similar mechanisms.

Liver fibrosis is the consequence of multiple factors, and may result in life threatening events, including various complications and hepatobiliary tumor. To block the process of liver and biliary fibrosis, there are

several strategies which can be implemented to block liver inflammation and the fibrosis process which mostly focus on anti-viral therapies for viral hepatitis. However, advanced fibrosis and cirrhosis cannot be well reversed by anti-viral therapies. The understanding of liver fibrosis and its mechanisms remains more important for the purpose of treatment. The present study aimed to clarify the role of miR-21 and associated cytokines in the process.

MiRNAs are a class of non-coding molecules, found to regulate a variety of cellular functions in health and disease, with the dysregulation of microRNAs being involved in several diseases, particularly liver disease and hepatocarcinogenesis. Most studies have demonstrated that miR-21 plays a role in protecting the liver from injury and damage. In a mouse study, miR-21 ablation ameliorated liver damage in BDL mice, implying that the expression of miR-21 could have a role in cholestasis.[29] However, the same study also showed that miR-21 seemed not to play a role in the prevention of liver cancer and fibrosis.[30] Kennedy et al. demonstrated that mice lacking miR-21 could increase Smad-7 expression, resulting in biliary hyperplasia and hepatic fibrosis.[31] Thus, there may be clues that over expressed miR-21 could lead to increased biliary proliferation and hepatic fibrosis in cholestatic type liver injury.

Liver fibrosis results from persistent and chronic injuries, often resulting in cirrhosis and liver tumor. MiR-21 is also considered as playing a critical role in the production of pro-inflammatory cytokines in the liver. In the present study, we performed rat cytokine arrays, with TIMP-1 being the most related cytokine in BDL rats. The cytokine TIMP-1, which is mostly up-regulated in our cytokine array, may play a role in the process of liver fibrosis or tumorigenesis. A previous study demonstrated that TIMP-1 does not by itself result in liver fibrosis, but does strongly promote liver fibrosis development.[32] However, the role of TIMP-1 was not clarified, and TIMP-1 was found upregulated, but not essential for hepatic fibrogenesis and carcinogenesis in mice.[33] miR-21 upregulated TIMP-1 was closely associated with fibrosis in a rat model with nonalcoholic steatohepatitis and lung fibrosis.[30, 34]

Our results show the role of miR-21 in a CBDL rat model, with the drug effects also demonstrated. The miR-21 regulated TIMP-1 or its association has potential in playing both a diagnostic and therapeutic role in patients with fibrosis of the liver or other organs. However, the definite role of miR-21 and the associated mechanism has not been very clearly defined in the present study. In particular, the role of hepatic stellate cells, which are important in liver fibrosis and could be regulated by miR-21, has not been studied.[34-36]

MiR-21 offers a potential role in hepatofibrosis and tumogenesis, and would have both a diagnostic and therapeutic role in both processes. There are several targets which have been reported via different functional mechanisms regulated by miR-21. Several medications have a potential role to play in the primary prevention or treatment of liver fibrosis, and miR-21 may therefore be affected. There could be a hint in miR-21 associated targets and any drugs involved surrounding the diagnostic and therapeutic treatment of chronic liver diseases and any complications which may occur.

Declarations

Conflict of interest

The authors declare that they have no conflicted interest.

Ethical approval

All procedures performed in studies involving human participants were in accordance with the ethical standards of the institutional and with the 1964 Helsinki Declaration and its later amendments or comparable ethical standards.

Acknowledgement

The authors would like to thank Taichung Veterans General Hospital for their support under a research grant (TCVGH-1053304C, TCVGH-1063304C).

Informed consent

Not applicable.

Data availability statements

The datasets generated during and/or analysed during the current study are available from the corresponding author on reasonable request.

Authors' contributions

Yen-Chung Peng (45%) designed, conducted and supervised experiments and contributed to manuscript preparation; Chung-Hsin Lee (25%) designed, conducted and supervised experiments and contributed to manuscript preparation; Yi-Chin Yang (15%) and Yi-Wen Hung (10%) conducted basic study research work; Ching-Chang Cheng (5%) contributed to manuscript preparation and Statistical Analysis.

References

1. Bataller R and Brenner DA (2005) Liver fibrosis. *J Clin Invest* 115:209-18. doi: 10.1172/JCI24282
2. Cabrera-Rubio R, Patterson AM, Cotter PD and Beraza N (2019) Cholestasis induced by bile duct ligation promotes changes in the intestinal microbiome in mice. *Sci Rep* 9:12324. doi: 10.1038/s41598-019-48784-z
3. Hernandez-Gea V and Friedman SL (2011) Pathogenesis of liver fibrosis. *Annu Rev Pathol* 6:425-56. doi: 10.1146/annurev-pathol-011110-130246
4. Zhou WC, Zhang QB and Qiao L (2014) Pathogenesis of liver cirrhosis. *World J Gastroenterol* 20:7312-24. doi: 10.3748/wjg.v20.i23.7312
5. Hargrove L, Kennedy L, Demieville J, Jones H, Meng F, DeMorrow S, Karstens W, Madeka T, Greene J, Jr. and Francis H (2017) Bile duct ligation-induced biliary hyperplasia, hepatic injury, and fibrosis are

- reduced in mast cell-deficient Kit(W-sh) mice. *Hepatology* 65:1991-2004. doi: 10.1002/hep.29079
6. Page-McCaw A, Ewald AJ and Werb Z (2007) Matrix metalloproteinases and the regulation of tissue remodelling. *Nat Rev Mol Cell Biol* 8:221-33. doi: 10.1038/nrm2125
 7. Tag CG, Sauer-Lehnen S, Weiskirchen S, Borkham-Kamphorst E, Tolba RH, Tacke F and Weiskirchen R (2015) Bile duct ligation in mice: induction of inflammatory liver injury and fibrosis by obstructive cholestasis. *J Vis Exp*. doi: 10.3791/52438
 8. Thiele ND, Wirth JW, Steins D, Koop AC, Ittrich H, Lohse AW and Kluwe J (2017) TIMP-1 is upregulated, but not essential in hepatic fibrogenesis and carcinogenesis in mice. *Sci Rep* 7:714. doi: 10.1038/s41598-017-00671-1
 9. Wu L, Luo Z, Zheng J, Yao P, Yuan Z, Lv X, Zhao J and Wang M (2018) IL-33 Can Promote the Process of Pulmonary Fibrosis by Inducing the Imbalance Between MMP-9 and TIMP-1. *Inflammation* 41:878-885. doi: 10.1007/s10753-018-0742-6
 10. Xu H, Zhang S, Pan X, Cao H, Huang X, Xu Q, Zhong H and Peng X (2016) TIMP-1 expression induced by IL-32 is mediated through activation of AP-1 signal pathway. *Int Immunopharmacol* 38:233-7. doi: 10.1016/j.intimp.2016.06.002
 11. Baek S, Cho KJ, Ju HL, Moon H, Choi SH, Chung SI, Park JY, Choi KH, Kim DY, Ahn SH, Han KH and Ro SW (2015) Analysis of miRNA expression patterns in human and mouse hepatocellular carcinoma cells. *Hepatol Res* 45:1331-40. doi: 10.1111/hepr.12510
 12. Lendvai G, Kiss A, Kovalszky I and Schaff Z (2012) [MicroRNAs in hepatocarcinogenesis]. *Orv Hetil* 153:978-89. doi: 10.1556/OH.2012.29387
 13. Zhou J, Yu L, Gao X, Hu J, Wang J, Dai Z, Wang JF, Zhang Z, Lu S, Huang X, Wang Z, Qiu S, Wang X, Yang G, Sun H, Tang Z, Wu Y, Zhu H and Fan J (2011) Plasma microRNA panel to diagnose hepatitis B virus-related hepatocellular carcinoma. *J Clin Oncol* 29:4781-8. doi: 10.1200/JCO.2011.38.2697
 14. Karakatsanis A, Papaconstantinou I, Gazouli M, Lyberopoulou A, Polymeneas G and Voros D (2013) Expression of microRNAs, miR-21, miR-31, miR-122, miR-145, miR-146a, miR-200c, miR-221, miR-222, and miR-223 in patients with hepatocellular carcinoma or intrahepatic cholangiocarcinoma and its prognostic significance. *Mol Carcinog* 52:297-303. doi: 10.1002/mc.21864
 15. Bauersachs J (2012) miR-21: a central regulator of fibrosis not only in the broken heart. *Cardiovasc Res* 96:227-9; discussion 230-3. doi: 10.1093/cvr/cvs200
 16. Chen J, Yu Y, Li S, Liu Y, Zhou S, Cao S, Yin J and Li G (2017) MicroRNA-30a ameliorates hepatic fibrosis by inhibiting Beclin1-mediated autophagy. *J Cell Mol Med* 21:3679-3692. doi: 10.1111/jcmm.13278
 17. Dongiovanni P, Meroni M, Longo M, Fargion S and Fracanzani AL (2018) miRNA Signature in NAFLD: A Turning Point for a Non-Invasive Diagnosis. *Int J Mol Sci* 19. doi: 10.3390/ijms19123966
 18. Feili X, Wu S, Ye W, Tu J and Lou L (2018) MicroRNA-34a-5p inhibits liver fibrosis by regulating TGF-beta1/Smad3 pathway in hepatic stellate cells. *Cell Biol Int* 42:1370-1376. doi: 10.1002/cbin.11022
 19. Hyun J, Wang S, Kim J, Rao KM, Park SY, Chung I, Ha CS, Kim SW, Yun YH and Jung Y (2016) MicroRNA-378 limits activation of hepatic stellate cells and liver fibrosis by suppressing Gli3

- expression. *Nat Commun* 7:10993. doi: 10.1038/ncomms10993
20. Vasuri F, Visani M, Acquaviva G, Brand T, Fiorentino M, Pession A, Tallini G, D'Errico A and de Biase D (2018) Role of microRNAs in the main molecular pathways of hepatocellular carcinoma. *World J Gastroenterol* 24:2647-2660. doi: 10.3748/wjg.v24.i25.2647
 21. Liao Q, Han P, Huang Y, Wu Z, Chen Q, Li S, Ye J and Wu X (2015) Potential Role of Circulating microRNA-21 for Hepatocellular Carcinoma Diagnosis: A Meta-Analysis. *PLoS One* 10:e0130677. doi: 10.1371/journal.pone.0130677
 22. Shen KH, Hung JH, Chang CW, Weng YT, Wu MJ and Chen PS (2017) Solasodine inhibits invasion of human lung cancer cell through downregulation of miR-21 and MMPs expression. *Chem Biol Interact* 268:129-135. doi: 10.1016/j.cbi.2017.03.005
 23. Takeuchi-Yorimoto A, Yamaura Y, Kanki M, Ide T, Nakata A, Noto T and Matsumoto M (2016) MicroRNA-21 is associated with fibrosis in a rat model of nonalcoholic steatohepatitis and serves as a plasma biomarker for fibrotic liver disease. *Toxicol Lett* 258:159-167. doi: 10.1016/j.toxlet.2016.06.012
 24. Cheng CC, Lin NN, Lee YF, Wu LY, Hsu HP, Lee WJ, Tung KC and Chiun YT (2010) Effects of Shugan-Huayu powder, a traditional Chinese medicine, on hepatic fibrosis in rat model. *Chin J Physiol* 53:223-33. doi: 10.4077/cjp.2010.amk050
 25. Shen CC, Yang YC and Liu BS (2011) Large-area irradiated low-level laser effect in a biodegradable nerve guide conduit on neural regeneration of peripheral nerve injury in rats. *Injury* 42:803-13. doi: 10.1016/j.injury.2011.02.005
 26. Ruwart MJ, Wilkinson KF, Rush BD, Vidmar TJ, Peters KM, Henley KS, Appelman HD, Kim KY, Schuppan D and Hahn EG (1989) The integrated value of serum procollagen III peptide over time predicts hepatic hydroxyproline content and stainable collagen in a model of dietary cirrhosis in the rat. *Hepatology* 10:801-6. doi: 10.1002/hep.1840100509
 27. Hsu LW, Goto S, Nakano T, Lai CY, Lin YC, Kao YH, Chen SH, Cheng YF, Jawan B, Chiu KW and Chen CL (2007) Immunosuppressive activity of serum taken from a liver transplant recipient after withdrawal of immunosuppressants. *Transpl Immunol* 17:137-46. doi: 10.1016/j.trim.2006.06.001
 28. Jonker AM, Dijkhuis FW, Boes A, Hardonk MJ and Grond J (1992) Immunohistochemical study of extracellular matrix in acute galactosamine hepatitis in rats. *Hepatology* 15:423-31. doi: 10.1002/hep.1840150312
 29. Afonso MB, Rodrigues PM, Simao AL, Gaspar MM, Carvalho T, Borralho P, Banales JM, Castro RE and Rodrigues CMP (2018) miRNA-21 ablation protects against liver injury and necroptosis in cholestasis. *Cell Death Differ* 25:857-872. doi: 10.1038/s41418-017-0019-x
 30. Caviglia JM, Yan J, Jang MK, Gwak GY, Affo S, Yu L, Olinga P, Friedman RA, Chen X and Schwabe RF (2018) MicroRNA-21 and Dicer are dispensable for hepatic stellate cell activation and the development of liver fibrosis. *Hepatology* 67:2414-2429. doi: 10.1002/hep.29627
 31. Kennedy LL, Meng F, Venter JK, Zhou T, Karstens WA, Hargrove LA, Wu N, Kyritsi K, Greene J, Invernizzi P, Bernuzzi F, Glaser SS, Francis HL and Alpini G (2016) Knockout of microRNA-21 reduces

- biliary hyperplasia and liver fibrosis in cholestatic bile duct ligated mice. *Lab Invest* 96:1256-1267. doi: 10.1038/labinvest.2016.112
32. Yoshiji H, Kuriyama S, Miyamoto Y, Thorgeirsson UP, Gomez DE, Kawata M, Yoshii J, Ikenaka Y, Noguchi R, Tsujinoue H, Nakatani T, Thorgeirsson SS and Fukui H (2000) Tissue inhibitor of metalloproteinases-1 promotes liver fibrosis development in a transgenic mouse model. *Hepatology* 32:1248-54. doi: 10.1053/jhep.2000.20521
33. Wei J, Feng L, Li Z, Xu G and Fan X (2013) MicroRNA-21 activates hepatic stellate cells via PTEN/Akt signaling. *Biomed Pharmacother* 67:387-92. doi: 10.1016/j.biopha.2013.03.014
34. Kitano M and Bloomston PM (2016) Hepatic Stellate Cells and microRNAs in Pathogenesis of Liver Fibrosis. *J Clin Med* 5. doi: 10.3390/jcm5030038
35. Trebicka J, Hennenberg M, Odenthal M, Shir K, Klein S, Granzow M, Vogt A, Dienes HP, Lammert F, Reichen J, Heller J and Sauerbruch T (2010) Atorvastatin attenuates hepatic fibrosis in rats after bile duct ligation via decreased turnover of hepatic stellate cells. *J Hepatol* 53:702-12. doi: 10.1016/j.jhep.2010.04.025
36. Zhang T, Yang Z, Kusumanchi P, Han S and Liangpunsakul S (2020) Critical Role of microRNA-21 in the Pathogenesis of Liver Diseases. *Front Med (Lausanne)* 7:7. doi: 10.3389/fmed.2020.00007

Tables

Table 1. Biochemical tests of CBDL rats with different assignment of drug treatment

n Week 1 after CBDL <i>P</i> value ^a				
		mean	± SD	
SGOT (IU/L)				0.475
Sham	6	106.67	± 13.20	
Sham + Aiodarone	6	121.33	± 21.04	
Sham + Simvastatin	6	135.50	± 69.02	
CBDL	6	347.17	± 131.61	
CBDL + Amiodarone	6	559.67	± 248.62	
CBDL + Simvastatin	6	198.25	± 202.65	
SGPT (IU/L)				0.932
Sham	6	40.50	± 4.76	
Sham + Aiodarone	6	47.00	± 4.43	
Sham + Simvastatin	6	38.83	± 9.50	
CBDL	6	92.17	± 22.87	
CBDL + Amiodarone	6	155.17	± 76.05	
CBDL + Simvastatin	6	71.25	± 44.85	
ALK-Pase (U/L)				< 0.001**
Sham	6	274.17	± 50.91	
Sham + Amiodarone	6	318.83	± 39.99	
Sham + Simvastatin	6	274.17	± 75.94	
CBDL	6	432.83	± 106.59	
CBDL + Amiodarone	6	449.00	± 64.02	
CBDL + Simvastatin	6	430.50	± 142.24	

	n	Week 1 after CBDL	<i>P</i> value ^a	
		mean ± SD		
T-Bilirubin (mg/dl)				0.021*
Sham	6	0.01 ± 0.01		
Sham + Aiodarone	6	0.00 ± 0.01		
Sham + Simvastatin	6	0.01 ± 0.01		
CBDL	6	6.61 ± 3.42		
CBDL + Amiodarone	6	5.53 ± 3.15		
CBDL + Simvastatin	6	2.38 ± 3.08		
Creatinine (mg/dl)				< 0.001**
Sham	6	0.38 ± 0.04		
Sham + Aiodarone	6	0.43 ± 0.05		
Sham + Simvastatin	6	0.40 ± 0.00		
CBDL	6	0.37 ± 0.05		
CBDL + Amiodarone	6	0.42 ± 0.04		
CBDL + Simvastatin	6	0.40 ± 0.00		

a *P* values are determined by Repeated Measures ANOVA test.

Table 2. A summary of pathological examinations of hepatic tissue sections in the present study

a The value is determined by the sum of 3 different part of liver sections, n = 6 in each group.

b Statistic significance is determined by the Wilcoxon rank sum test, compare to the non-treated CBDL group

Pathology/ Degree	Groups/degree of severity, medium (LQ-UQ) ^a					
	Sham	Sham + AMI	Sham + Statin	CBDL	CBDL + AMI	CBDL + Statin
Proliferation and fibrosis (<i>P</i> value ^b)	□	□	□	4 (3.63 - 4.4)	6.5 (3.1 - 7.3) <i>P</i> = 0.485	3 (2.5 - 3.25) <i>P</i> = 0.038
Necrosis	□	□	□	0 (0 - 0.8)	□	0 (0 - 0.75)
Hepatocytic degeneration	□	□	□	0.5 (0 - 1.8)	□	□

Figures

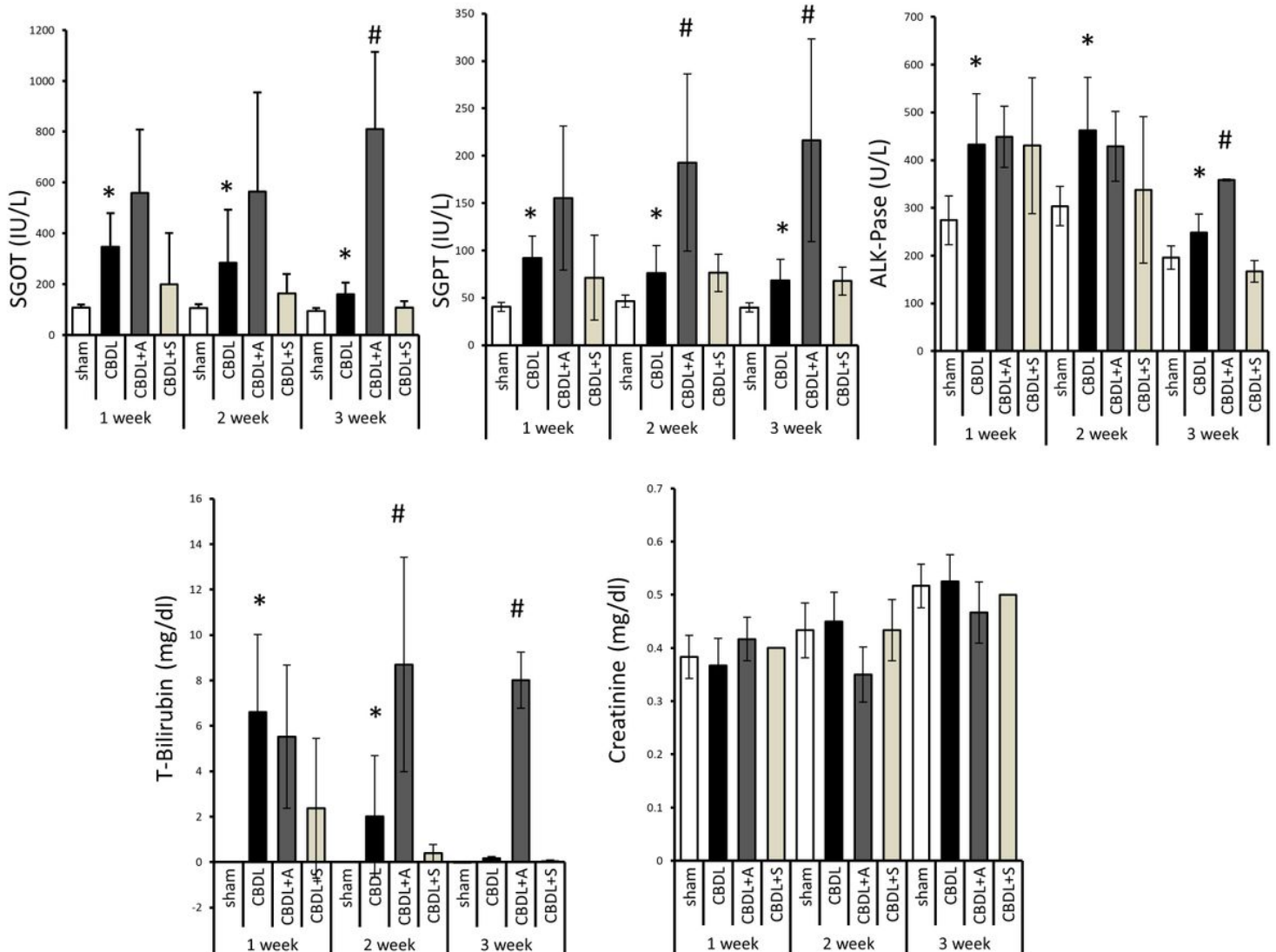


Figure 1

Biochemical analysis of serum indicators in CBDL rats The activity of serum GOT, GPT and ALK-Pase and the level of serum Bilirubin and creatinine were determined through biochemical analysis. The rat's blood samples were harvested at 1, 2, and 3 week intervals after CBDL surgery. * indicates $P < 0.05$ when comparing the CBDL group with the SHAM group; # indicates $P < 0.05$ when comparing CBDL + the amiodarone group with the CBDL group. The statistical significances were determined by a one-way ANOVA test (n = 6).

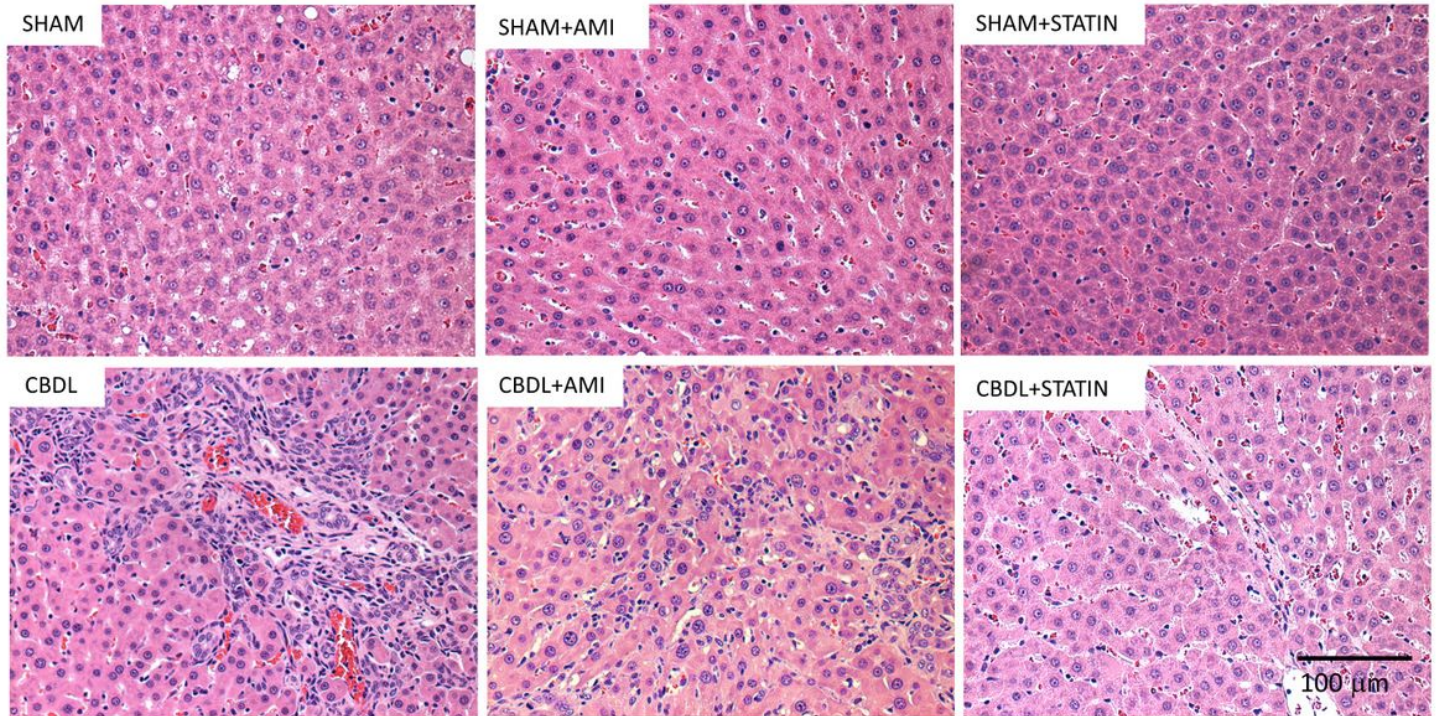


Figure 2

Histological examination of hepatic tissue from experimental rats Based on the results from HE stain, cell proliferation and fibrosis are found in the CBDL groups, which resulted in scarring and thickening of liver tissue. Mild hemorrhage and necrosis also existed in the CBDL-only group.

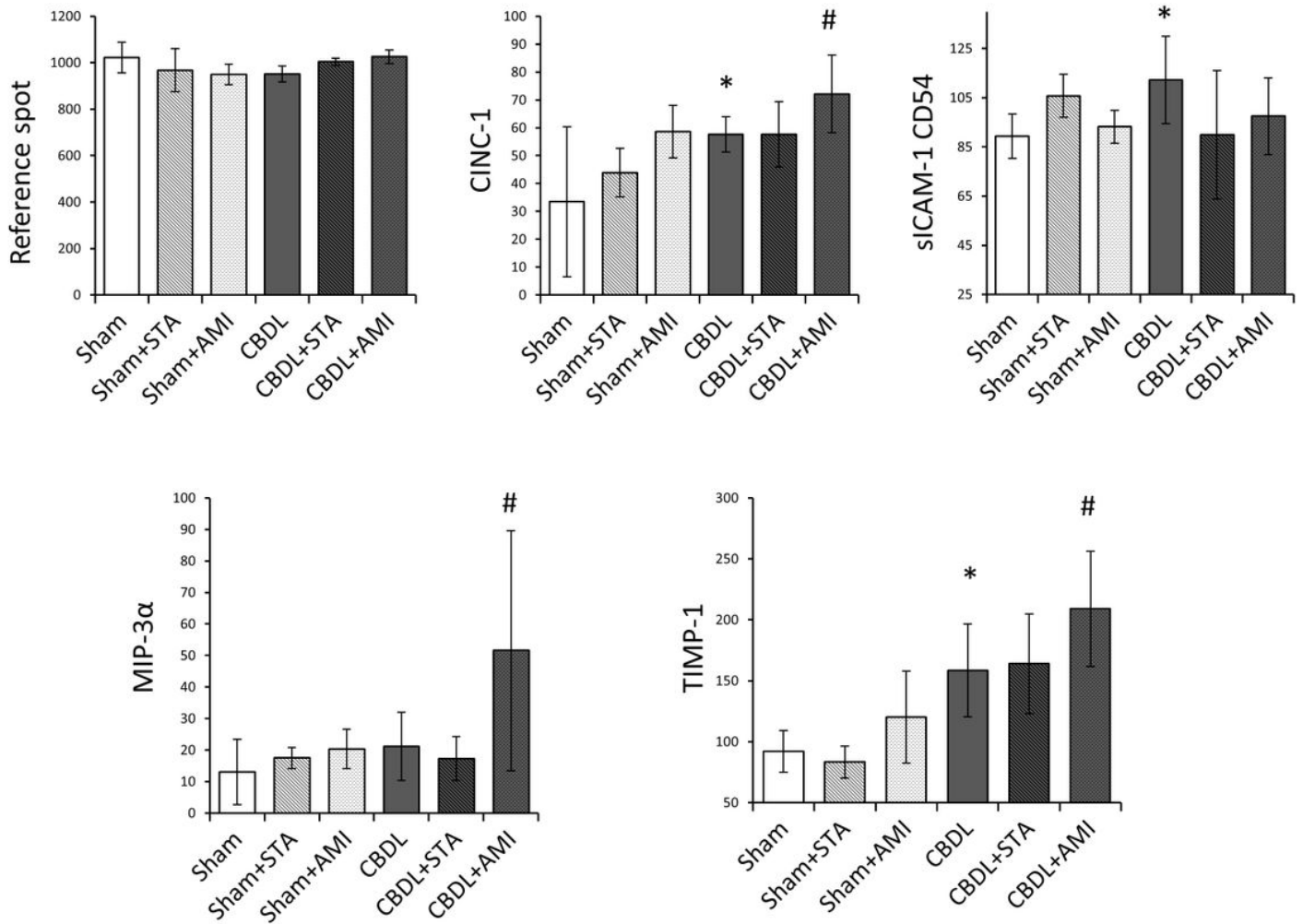


Figure 3

Analysis of functional cytokines in CBDL rats Serum samples from experimental animals were harvested at 21 days after CBDL. Twenty-nine factors with 3 reference spots and one negative control spot were loaded on a single chip for 1 set of array, and 6 independent chips were performed. * indicates $P < 0.05$ when comparing the CBDL group with the SHAM group; # indicates $P < 0.05$ when comparing the CBDL + amiodarone group with the SHAM group. The statistical significances were determined by a one-way ANOVA test ($n = 6$). CINC-1: Cytokine-induced neutrophil chemoattractant 1; sICAM-1: Intercellular Adhesion Molecule 1; MIP-3α: Macrophage Inflammatory Protein-3α or CCL20.

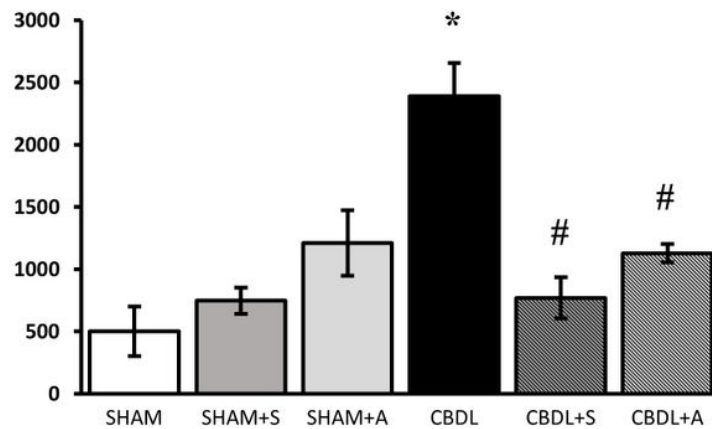
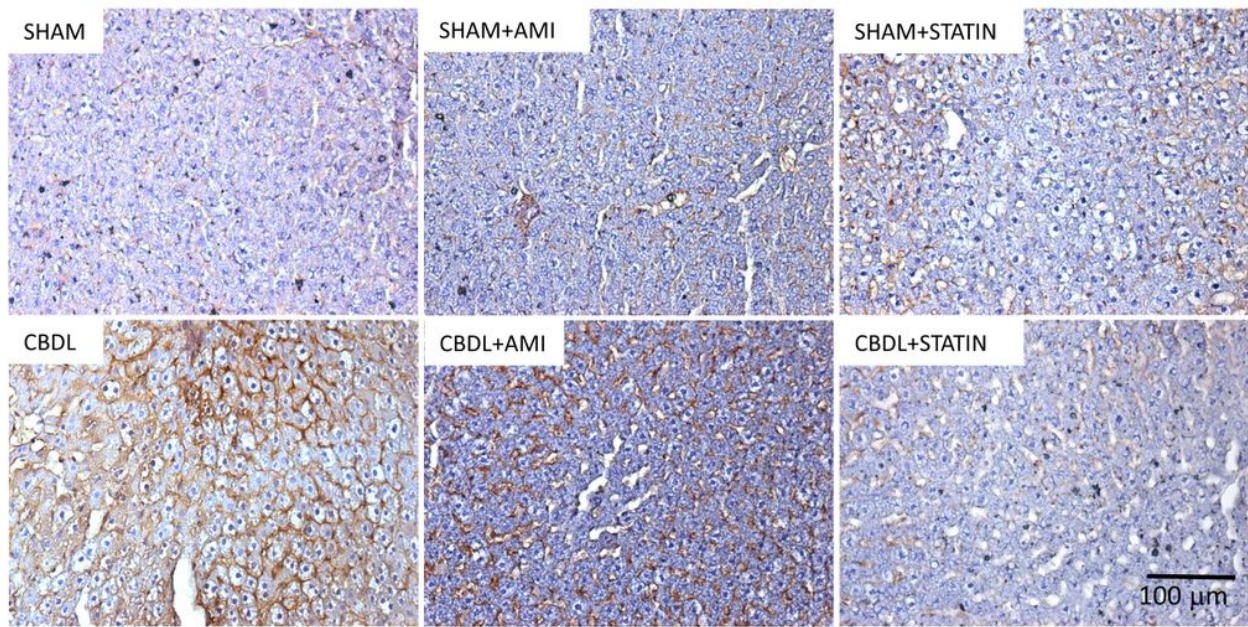


Figure 4

Histological assessment of TIMP-1 expression. Immunohistological stains were performed using the primary antibody against TIMP-1. The color reaction was performed using Diaminobenzidine which can be visualized through phase contrast light microscopy in brown color. TIMP-1 mainly localized in cytosol and the extracellular space of liver tissue. The TIMP-1-positive area was quantified and is shown in the lower panel. * indicates $P < 0.05$ when comparing the CBDL group with the SHAM group; # indicates $P < 0.05$ when comparing either the CBDL + amiodarone or CBDL + simvastatin group with the CBDL group. The statistical significances were determined by a one-way ANOVA test ($n = 6$).

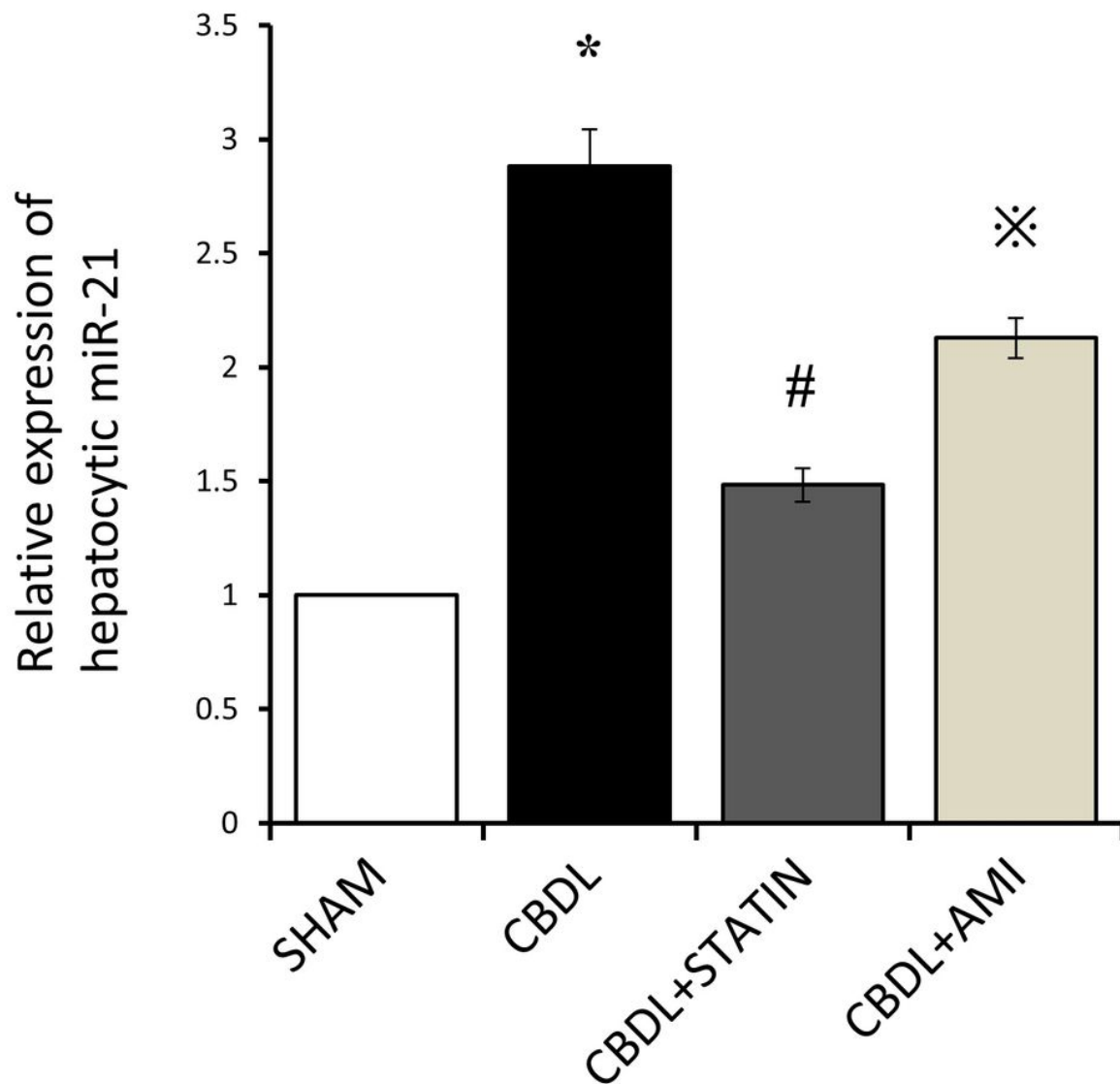


Figure 5

Assessment of miR-21 expression by Taqman microRNA assay Small RNA from liver samples in each group was used to performed microRNA assay. U6 small nuclear RNA was used as an internal control. DATA was presented by relative fluorescent intensity ($2^{-(\Delta\Delta Ct)}$). * indicates $P < 0.05$ when comparing the CBDL group with the SHAM group; # indicates $P < 0.05$ when comparing the CBDL + simvastatin group with the CBDL group; ⊗ indicates $P < 0.05$ when comparing the CBDL + simvastatin group with the CBDL + amiodarone group. The statistical significances were determined by a one-way ANOVA test ($n = 6$).